Supplemental Figures

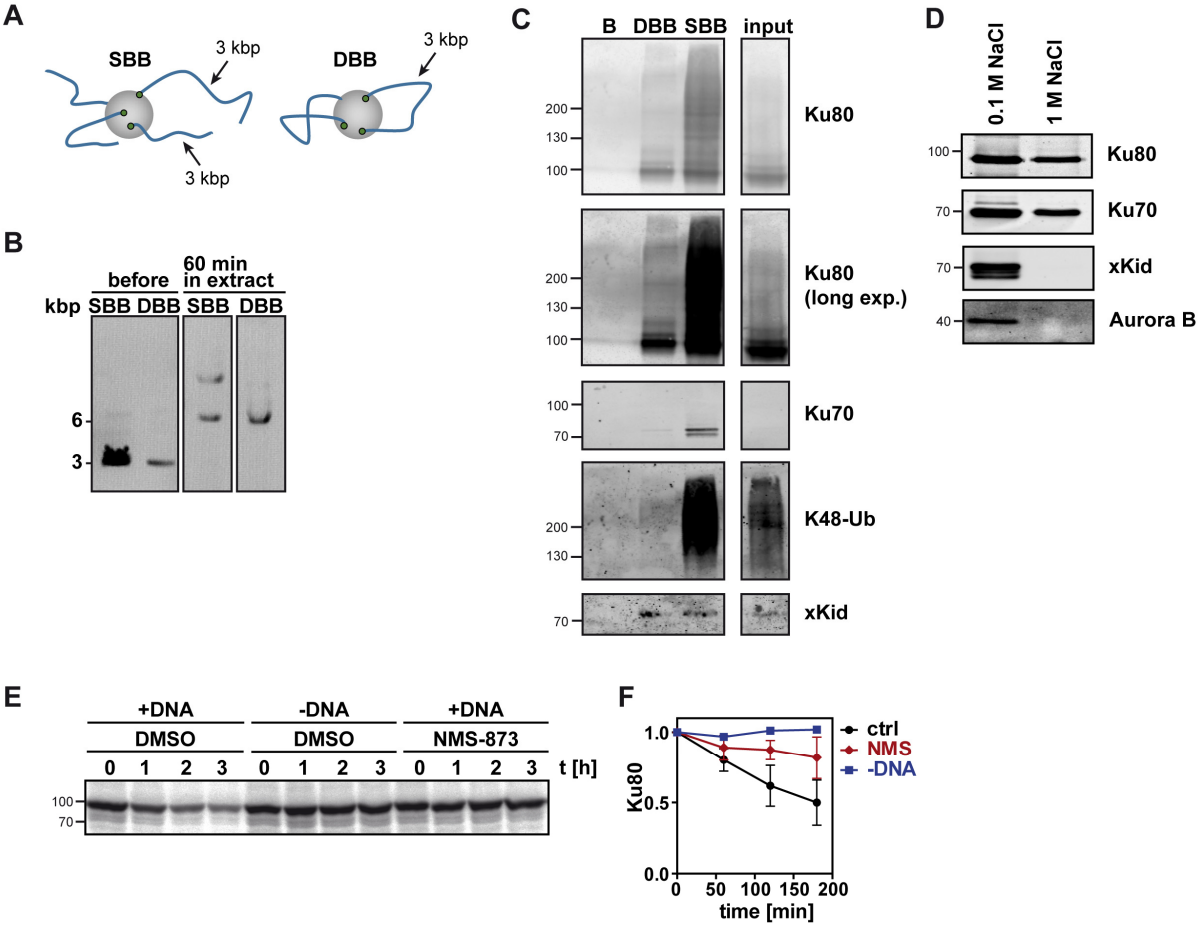

Figure S1. Characterisation of DNA beads. Related to Figure 1.

A Schematic of SB-DNA beads (SBB) and DB-DNA beads (DBB). For SB-DNA beads, 3 kilobase pairs (kbp) linear DNA was biotinylated on one end and immobilised on magnetic streptavidin dynabeads such that free DNA ends emanated from beads. For DB-DNA beads, both DNA ends of the 3kbp fragment were biotinylated and immobilised.

B SB-DNA beads and DB-DNA beads were incubated in egg extract for 60 min or analysed before incubation as indicated before. Length of DNA fragments was analysed by agarose gel electrophoresis. Note that the 3 kbp DNA on the SB-DNA beads, but not on DB-DNA beads, is ligated by DNA repair, yielding a band at 6 kbp.

C SB-DNA (SBB), DB-DNA (DBB), or streptavidin beads alone (B) were incubated in egg extract for 30 min, reisolated and bound proteins were detected by Western blot with indicated antibodies.

D A large fraction of Ku on SB-DNA beads is salt resistant. SB-DNA beads were incubated in egg extract supplemented with 8 µM p97-ND1 for 1 h at 22 °C. Beads were washed in CSF-XB buffer containing either 100 mM NaCl or 1 M NaCl. Bound proteins were eluted in SDS sample buffer and analysed by Western blot. The high-affinity DNA binding protein xKid and Aurora B were used as controls.

E p97 activity is required for Ku80 degradation associated with DSB repair. 600 µg/ml linear DNA or buffer alone (-DNA) was added to extracts supplemented with ^{35}S-Ku80. Reactions were carried out in the presence of an allosteric p97 inhibitor (NMS-873; 20 µM) or DMSO alone as indicated.

F Quantification of E. Remaining Ku80 was normalised to t_0. Mean ± sd from three independent experiments.

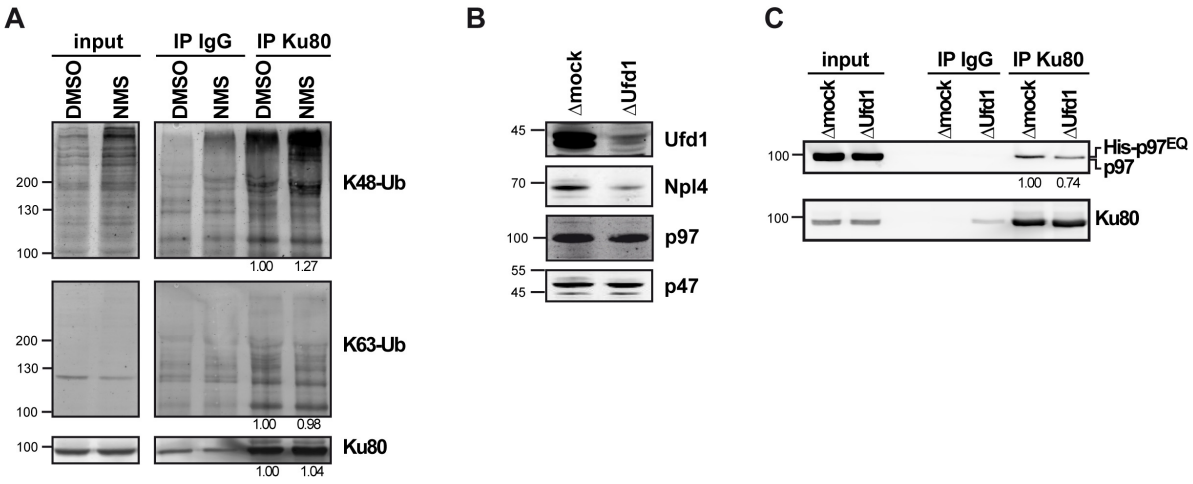

Figure S2. Accumulation of K48 ubiquitin upon p97 inhibition and effects of Ufd1 depletion on Ku80 binding by p97. Related to Figure 2.

A K48-ubiquitinated Ku80 accumulates when p97 is compromised. Extracts were supplemented with linear DNA, and p97 inhibitor (NMS-873; 20 μM) or DMSO alone. Extracts were incubated for 1 h prior to immunoprecipitation (IP) with Ku80 or control antibodies as indicated. Western blot with K48 and K63 chain-specific ubiquitin antibodies and Ku80 as IP control. Signal intensities were quantified and normalized to control.

B Ufd1 depletion in egg extract. Extracts were immunodepleted with a Ufd1-specific monoclonal antibody and probed by Western blot.

C Ufd1 depletion reduces p97 interaction with Ku80. Extracts were either Ufd1-depleted (ΔUfd1) or mock-depleted (Δmock) and supplemented with 0.33 μM p97-EQ and 600 μg/ml linear DNA. After incubation (30 min at 22 °C), Ku80 was immunoprecipitated and co-precipitated p97 was analysed by Western blot. Signal intensities are displayed relative to the Δmock sample after normalisation to p97 input levels.

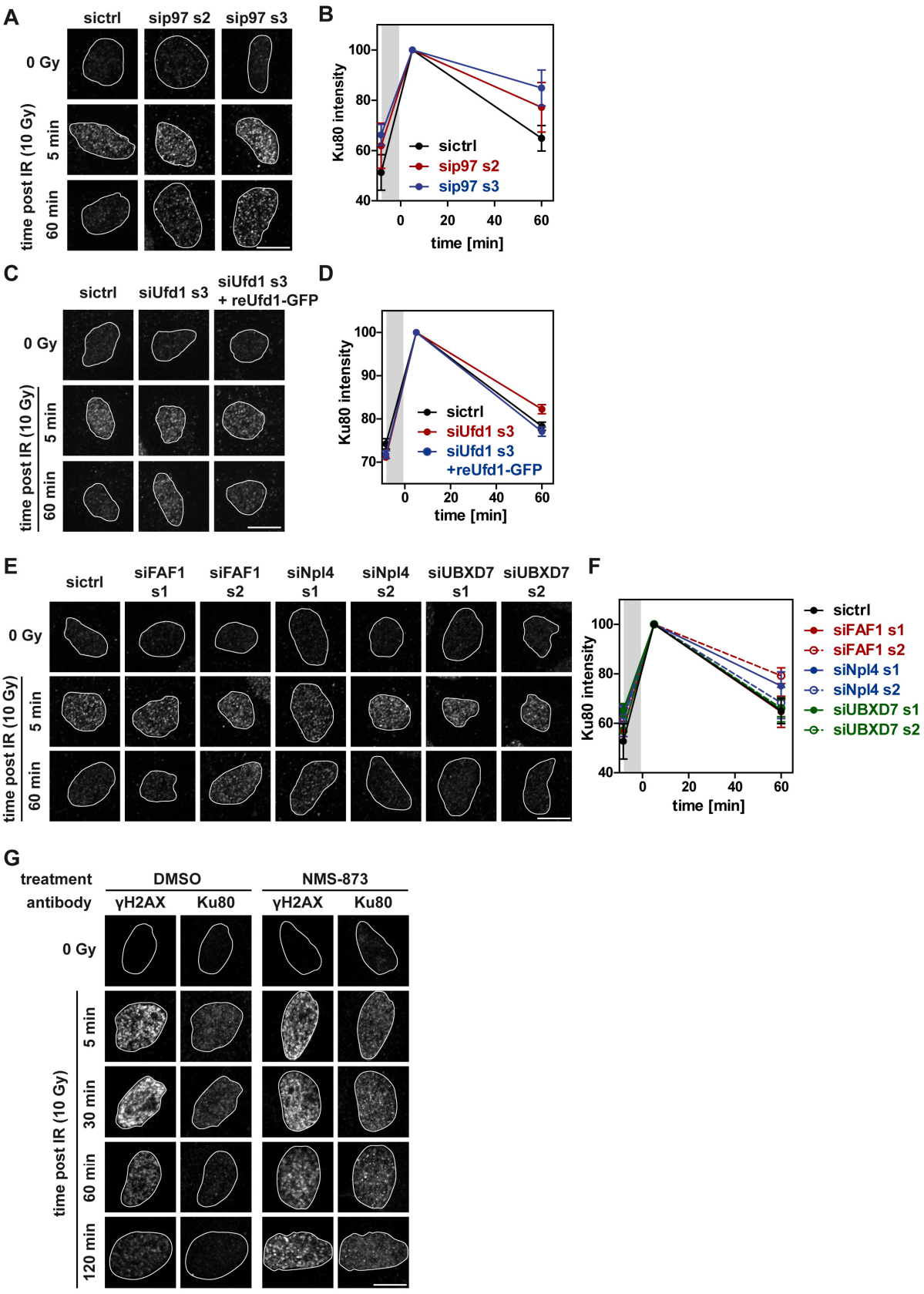

Figure S3. Cellular Ku80 release assay with additional siRNAs. Related to Figure 3.

A Effect of p97 depletion by 2 additional siRNAs in Ku80 foci assay. Representative images as in Figure 3E.

B Mean Ku80 signal intensity in the nucleus was quantified by automated image analysis and normalised to t_5 as in Figure 3F. Mean ± sd; n = 3 independent experiments with at least 50 cells per condition. Gray area indicates the time of irradiation.

C Effect of Ufd1 depletion by an additional siRNA and rescue by overexpression of an siRNA-resistant Ufd1-GFP (reUfd1-GFP) in Ku80 foci assay. Representative images as in Figure 3E.

D Automated image quantification of C. Mean ± sem; n > 150 cells of 3 independent experiments.

E Effects of depletions of additional p97 adapter proteins. U2OS cells were treated with control siRNA (sictrl), or siRNA targeting FAF1, Npl4 or UBXD7. Cells were irradiated with 10 Gy or mock treated (0 Gy), and collected at indicated times for visualization of chromatin-bound Ku80 as in Figure 3E.

F Automated image quantification of E. Mean ± sd; n = 3 independent experiments with at least 50 cells per condition.

G γH2AX persists upon p97 inhibition. Representative images of γH2AX and Ku80 intensity in the cell-based Ku80 chromatin release assay (some of the images shown here were also used as representative images in Figure 3C).

All scale bars: 10 μm.

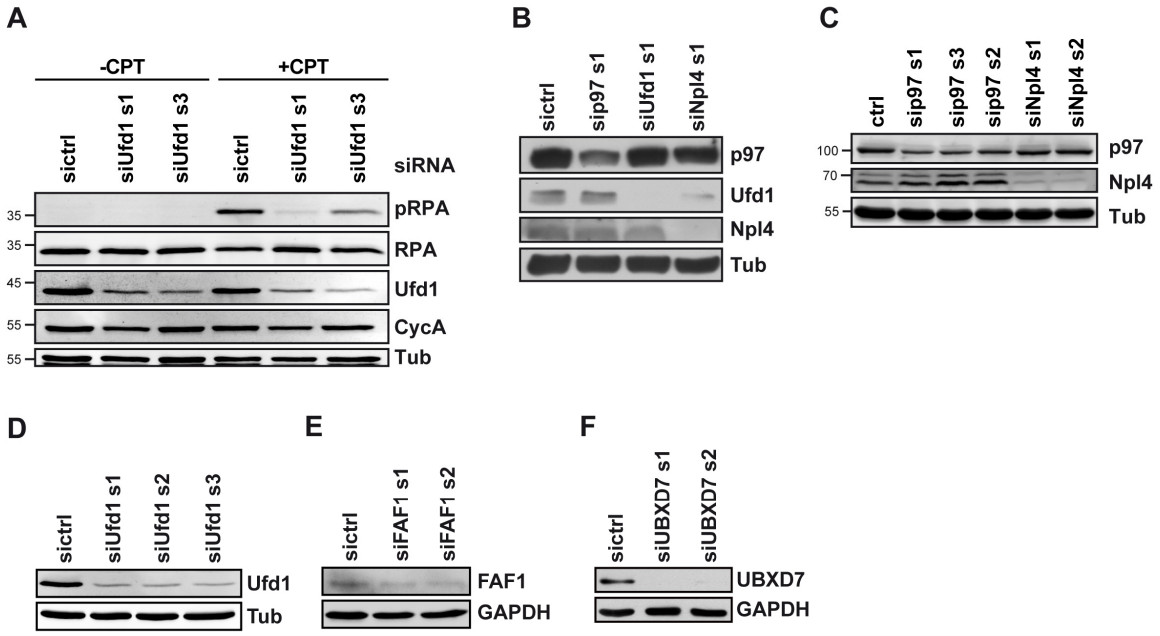

Figure S4. Effects of additional Ufd1 siRNA on phospho-RPA (pRPA) and depletion efficiencies of siRNAs. Related to Figure 4.

A Effect of additional Ufd1 siRNA on phospho-RPA (pRPA). Immunoblot analysis of cells treated with camptothecin (+CPT) or DMSO (-CPT) as in Figure 4D after siRNA-mediated depletion of Ufd1.

B Depletion efficiencies of siRNAs used in Figure 3E were determined by Western blot with indicated antibodies.

C Depletion efficiencies of siRNAs targeting p97 or Npl4 used in this study were determined by Western blot with indicated antibodies.

D Depletion efficiencies of siRNAs targeting Ufd1 used in this study were determined by Western blot with indicated antibodies.

E Depletion efficiencies of siRNAs targeting FAF1 used in this study were determined by Western blot with indicated antibodies.

F Depletion efficiencies of siRNAs targeting UBXD7 used in this study were determined by Western blot with indicated antibodies.

Supplemental Tables

Table S1. Related to Figure 1. List of proteins isolated on SB-DNA beads detected by mass spectrometry. Related to Figure 1.

Table S1 is attached as Excel file. The two sheets ("simple" and "extended") contain the same dataset, with a more detailed view in the "extended" sheet. The columns contain the following data:

Protein names: The full protein name of the identified protein, as recommended by the UniProt consortium.

Gene names: The name of the gene coding for the identified protein sequence, according to the UniProt database.

Label in Fig 1A: Indicates the name for the identified protein that is used in this study and was used for labeling in Fig 1A.

Protein IDs: Unique UniProt protein identifier(s) of the protein(s) contained in this group.

Majority protein IDs: UniProt protein identifier(s) of those proteins that have at least half of the peptides that the most abundant (leading) protein in this group has.

Peptides: Total number of peptide sequences identified for this protein.

Sequence coverage [%]: Percentage of the sequence covered by the identified peptides.

Score: The Andromeda (Cox et al. 2011) protein probability score which is derived from peptide posterior error probabilities. High value means high probability that the protein was assigned correctly.

MS/MS count: Sum of all peptide spectra matches for indicated protein.

Intensity: Sum of the eXtracted Ion Current (XIC) of all individual peptides associated with the identified protein.

Table S2. Related to Figure 1. Mass spectrometry list of proteins enriched or reduced upon addition of p97-ND1 displayed in Figure 1A. Related to Figure 1.

Table S2 is attached as Excel file. The two sheets ("simple" and "extended") contain the same dataset, with a more detailed view in the "extended" sheet. The columns contain the following data:

log2 (Difference): This value is plotted on the x axis in Fig 1A. The value indicates how much the respective protein is enriched (positive values) or reduced (negative values) on SB-DNA beads incubated in extracts with p97-ND1 compared to a sample without ND1 (n = 4).

-LOG(p-value): This value is plotted on the y axis in Fig 1A. Significance of the difference in the sample with and without p97-ND1 was tested with a two-sided t-test (n = 4).

Significance: The protein was tested for significant enrichment or reduction applying a 5% false discovery rate (FDR; s0 = 0.1).

Protein names: The full protein name of the identified protein, as recommended by the UniProt consortium.

Gene names: The name of the gene coding for the identified protein sequence, according to the UniProt database.

Label in Fig 1A: Indicates the name for the identified protein that is used in this study and was used for labeling in Fig 1A.

Protein IDs: Unique UniProt protein identifier(s) of the protein(s) contained in this group.

Majority protein IDs: UniProt protein identifier(s) of those proteins that have at least half of the peptides that the most abundant (leading) protein in this group has.

Peptides: Total number of peptide sequences identified for this protein.

Sequence coverage [%]: Percentage of the sequence covered by the identified peptides.

Score:

The Andromeda (Cox et al. 2011) protein probability score which is derived from peptide posterior error probabilities. High value means high probability that the protein was assigned correctly.

MS/MS count: Sum of all peptide spectra matches for indicated protein.

Intensity: Sum of the eXtracted Ion Current (XIC) of all individual peptides associated with the identified protein.

Supplemental Experimental Procedures

Antibodies and Proteins

Antibodies against p97 (HME 8), Ufd1 (5E2 for depletion and HME14 for Western blots), Npl4 (HME18), p47 (HME22), UBXD1 (E43), Aurora B, and xKid were used as described (Meyer et al. 2000; Hetzer et al. 2001; Funabiki und Murray 2000). Ku80 antibody (Ab-2 clone 111) was purchased from NeoMarkers. Monoclonal p97 antibody (10R-P104A) was purchased from Fitzgerald. Rad51 antibody (14B4) was from GeneTex. Antibody against RPA-1 (ABIN151627) and FAF1 (ABIN1988265) were from antikörper-online, antibodies against RPA2/3 (ab2175), γH2AX (ab11174), and cyclin A (6E6) were from Abcam; antibody against phosphorylated RPA2/3 (A300-245A) was from Biomol, antibody against UBXD7 (S409D) was from MRC-PPU Reagents. Mouse monoclonal antibody against p97 (10R-P104A) was purchased from Fitzgerald; antibody against tubulin (T-5168) was from Sigma-Aldrich. Antibody against GAPDH (G8795) was from Sigma. Antibodies against K48-linked (Apu2) or K63-linked (Apu3) ubiquitin chains were purchased from Millipore.

Human ubiquitin, ubiquitin^{K48R}, and ubiquitin^{K63R} was generated in bacteria as described (Wang et al. 2004). Ubiquitin^{K11R} and ubiquitin^{K0} (i. e. all lysines mutated to arginines) were purchased from Biomol.

Immunodepletions in Egg Extract

Ufd1 was immunodepleted, using 40 µg anti-Ufd1 antibody (5E2) bound to Protein G agarose (Merck-Millipore) for 100 µl extract. Ku80 was depleted as previously described (Postow und Funabiki 2014), using two rounds of 11.5 µg anti-xKu80 antibody per 50 µl extract. Antibodies were bound to Dynabeads protein G (Thermo Fisher Scientific) and removed after depletion using a magnet.

Ku80 Degradation Assay

Ku80 degradation was monitored as described previously (Postow et al. 2008). Briefly, pBluescript SK+ vector was digested with PvuII and SspI and added at a final concentration of 600 µg/µl to extract containing 35S-Ku80. Samples were taken at indicated times and analysed with a phosphoimager (Fujifilm).

pRPA Western Blot Assay

U2OS cells were pre-treated with siRNAs for 48 h or inhibitors for 15 min before DNA damage was induced with 1 µM camptothecin (CPT). After 1 h, cells were collected and lysed in lysis buffer (150 mM KCl, 5 mM MgCl2, 50 mM Tris-HCl pH 7.4, 1% Triton X-100, 5% Glycerol, 2 mM β-mercaptoethanol, Roche CompleteTM EDTA-free protease inhibitors, Roche PhosStopTM phosphatase inhibitors) for 20 min at 4 °C. The supernatant after centrifugation (17000 g; 10 min; 4 °C) was analysed by Western blot.

Immunofluorescence

Transfection and irradiation were described in Experimental Procedures. A Philips MCN 165 (3 mm Al filter; 130 kV, 16 mA; dose-rate 1.2 Gy/min) was used as X-ray source. Non-irradiated samples were treated with siRNA for 50 hours or with inhibitor for 120 minutes. For Ku80 and γH2AX staining, cells were pre-extracted in CSK buffer (10 mM Pipes, pH 7.0, 100 mM NaCl, 300 mM sucrose, 3 mM $MgCl_2$, 0.7% Triton X-100) containing RNase A (0.3 mg/ml; Britton et al. 2013). For staining of Rad51 or pRPA, no pre-extraction was performed. Cells were fixed with 4% formaldehyde in PBS for 15 min, washed with PBS and permeabilised for 10 min using 0.2% Triton X-100 in PBS. Samples were washed with

PBS and incubated in blocking solution (0.5% BSA, 0.2% gelatin in PBS) for 1 h followed by incubation with the indicated primary antibodies in blocking solution for 1 h. Coverslips were washed and incubated with fluorescently labeled secondary antibody conjugates for 1 h in blocking solution. Samples were washed with PBS and, if required, stained with DAPI (1 µg/ml). For SIM imaging, a post-fixation step with 2% formaldehyde for 10 min was added after incubation with secondary antibodies. After additional washing steps with PBS, coverslips were mounted using ProLong Gold antifade (Life Technologies) or Mowiol (VWR).

Microscopy and Image Analysis

Spinning disk confocal microscopy was performed on an Eclipse Ti-E (Nikon) inverted microscope with a Andor AOTF Laser Combiner, a CSU-X1 Yokogawa spinning disk unit and a iXon3 897 single photon detection EMCCD camera (Andor Technology). Images were acquired using either a CFI Apo TIRF 100×/1.49 NA oil immersion objective or a CFI Plan Apo VC 20×/0.75 NA air objective (Nikon). Laser lines used for excitation of Alexa Fluor® 488 and DAPI were 488 nm and 405 nm, respectively. Acquisition was controlled by Andor IQ Software (Andor Technology). Confocal laser-scanning microscopy was performed on a TCS SP5 II system equipped with standard PMT detectors (detection of DAPI) as well as sensitive HyD detectors (detection of Ku80, γH2AX) (Leica Microsystems). Images were acquired with an HCX PL APO 63×/1.4 NA oil-immersion objective (Leica Microsystems. Lasers used for excitation were DPSS 561 nm (Alexa Fluor® 568), Ar 488 nm (Alexa Fluor® 488) and Diode 405 nm (DAPI). Image acquisition was controlled by LASAF software (Leica Microsystems). Structured illumination microscopy was performed on a Zeiss ELYRA PS.1 equipped with a PCO edge sCMOS camera under the control of ZEN black software (Zeiss). Images were acquired with an alpha Plan-Apo 100×/1.46 NA oil immersion objective (Zeiss). A 488 nm OPSL laser was used for the excitation of Alexa Fluor® 488-labeled Ku80.

Images were processed using ImageJ software (http://rsbweb.nih.gov/ij/) and Adobe Illustrator (Adobe Photosystems). Automated Image Analysis was performed with Cell Profiler (Carpenter et al. 2006) and pipelines are available upon request.

siRNAs and Plasmids

siRNA oligomers targeting p97s1 (AAGAUGGAUCUCAUUGACCUA; Raman et al. 2011), p97s2 (CAAUAAACGUUGGGUCAAA; Zhou et al. 2013), p97s3 (AAGUAGGGUAUGAUGACAUUG; Wojcik et al. 2004), Ufd1s1 (GUGGCCACCUACUCCAAAUUU; Dobrynin et al. 2011), Ufd1s2 (GGGC UACAAAGAACCCGAA; Dobrynin et al. 2011), Npl4s1 (CGUGGUGGAGGAUGAGAUUUU; Dobrynin et al. 2011), Npl4s2 (CGGAAGGUUGGCUGGAUAUUUUU), RNF138 (UAGAUAAAGAAACCCAAUAUU; Ismail et al. 2015), UBXD1 (UCAGAUACCACGUUGGUCCCU), FAF1s1 (CCACCUUCAUCAUCUA GUCUU; Park et al. 2007), FAF1s2 (GGAGAGACGUAACUCAACUUU), UBXD7s1 (CAGCUUGAA AGGAGUGUUUUU), UBXD7s2 (CAGCAGGUGCAUAUUCAUU), Rad51 (GGGAAUUAGUGAAGC CAAA; Meerang et al. 2011), and non-targeting control siRNA (UUCUCCGAACGUGUCACGUUU; Dobrynin et al. 2011) were purchased from Microsynth.

For overexpression of siRNA-resistant Ufd1, C-terminally EGFP-tagged Ufd1 in pEGFP-N3 vector was used (Clontech; Dobrynin et al. 2011).

Pulsed-field Gel Electrophoresis

To analyse repair kinetics of DSB, PFGE was performed in this study. In this technique, the number of DSB present in the cells is indirectly measured by the fraction of DNA released (FDR) out of the well into the lane. Cells were trypsinised and suspended in serum free, HEPES-buffered medium (20 mM Hepes, 5 mM NaHCO3) at a concentration of 6×106 cells/ml. Cells were then mixed with an equal volume of pre-warmed (50°C) 1% low-melting agarose (Bio-Rad, Munich, Germany), and the cell suspension was pipetted into 3 mm diameter glass tubes. Agarose was allowed to solidify in ice, it was extruded from the glass tube and cut into 5-mm long plugs, which were irradiated in a Petri dish.

After the collection, agarose plugs were lysed using standard high temperature lysis (HTL) protocol, agarose plugs were pretreated in lysis buffer (10 mM Tris-HCl, pH7.6, 50mMNaCl, 100 mM EDTA, 2% N-lauryl (NLS) and 0.2 mg/ml protease added just before use) at 4°C for 1 h, before lysis at 50°C for 18 h. Subsequently, plugs with lysed cells were washed with washing buffer (10 mM Tris-HCl, pH7.6, 50 mM NaCl, 100 mM EDTA) at 37°C for 2 h, and digested with RNA digesting buffer (10 mM Tris-HCl,

pH 7.6, 50 mM NaCl, 100 mM EDTA, and 0.1 mg/ml RNase, added just before use) at 37°C for 2 h. Buffer volume was adjusted to about ten plug volumes.

PFGE was carried out in gels cast with 0.5% molecular biology grade agarose (Bio-Rad), which was run in 0.5×TBE at 8°C for 40 h. For better separation of released DNA, the electric field was pulsed and set at 50 V (1.25 V/cm) for 900 s in the forward direction and 200 V (5.00 V/cm) for 75 s in the reverse direction. After running, the gel was stained for 4 h with 1.6 µg/ml Ethidium Bromide, and imaged using a fluorescence imager (Typhoon 9400, Molecular Dynamics, Germany). FDR was analysed using ImageQuant 5.2 (GE healthcare, Freiburg, Germany). All the data shown represent the mean and standard deviation calculated from 3 determinations in 1 experiment.

HRR Reporter Assay

U2OS DR-GFP cells (Gunn et al. 2011) were seeded in 6-well plates (200 000 cells per well) and depleted with indicated siRNAs (15 nM) using Lipofectamine RNAiMAX (Life Technologies). The next day, cells were transfected with an I-SceI expression plasmid (pRRL sEF1a HA.NLS.Sce(opt).T2A.IFP (Certo et al. 2011); 1 µg per well) using jetPRIME (Polyplus-transfection) and medium was changed 4 h after transfection. 72 h after transfection, cells were washed with PBS, trypsinised, neutralised with medium, centrifuged and resuspended in 400 µl PBS. Samples were analysed by flow cytometry on a MACSQuant VYB (Miltenyi Biotec) measuring side scatter, forward scatter and green fluorescence (488 nm laser and 525/50 nm band pass filter). 20,000 gated events (living cells and doublet excluded) were acquired and Kaluza 1.3 software (Beckman Coulter) was used for analysis. GFP fluorescence was quantified as percent of gated events and normalised to sictrl in three independent experiments.

Mass Spectrometry

Sample Preparation, Reduction/Alkylation and Tryptic Digestion. SB-DNA beads were incubated in egg extract supplemented with 8 µM p97 ND1 for 45 min at 22 °C. In order to release bound proteins from the magnetic beads and to degrade the DNA, samples were treated with benzonase nuclease (Merck-Millipore). Quadruplicates were performed from the same egg extract. After removal of the beads, the samples were transferred to fresh Eppendorf tubes (40 µL) and mixed with 8 M urea (50 µL) in 100 mM ammonium bicarbonate (ABC). The proteins were reduced by addition of DTT (10 mM final) and incubation at 37 °C for 30 min and subsequently alkylated by addition of iodoacetamide (IAM, 27 mM final) and incubation at 30 °C for 30 min. In order to quench excess IAM, we added more DTT to a final concentration of 30 mM. After this treatment, Lys-C (Wako Laboratory Chemicals, 100 ng) was added and the samples were incubated for 3 h at 37 °C. The samples were diluted to 25 mM ABC and 0.9 M urea. Sequencing grade Trypsin (Promega, 100 ng) was added and the samples were incubated over night at 37 °C while shaking. On the next morning, the samples were acidified by adding formic acid (FA; final 0.5% v/v).

Sample clean-up for LC-MS. Acidified tryptic digests were desalted on home-made C18 StageTips as described (Rappsilber et al. 2007). The tryptic digest of each sample (~400 µL) was passed over a 2 disc StageTip. After elution from the StageTips, samples were dried using a vacuum concentrator (Eppendorf) and the peptides were taken up in 0.1% formic acid solution (10 µL).

LC-MS/MS. Experiments were performed on an Orbitrap Elite instrument (Thermo, Michalski et al. 2012) that was coupled to an EASY-nLC 1000 liquid chromatography (LC) system (Thermo). The LC was operated in the one-column mode. The analytical column was a fused silica capillary (75 µm × 20 cm) with an integrated PicoFrit emitter (New Objective) packed in-house with Reprosil-Pur 120 C18-AQ 1.9 µm resin (Dr. Maisch). The analytical column was encased by a column oven (Sonation) and attached to a nanospray flex ion source (Thermo). The column oven temperature was adjusted to 45 °C during data acquisition and in all other modi at 30 °C. The LC was equipped with two mobile phases: solvent A (0.1% formic acid, FA, in water) and solvent B (0.1% FA in acetonitrile, ACN). All solvents were of UPLC grade (Sigma). Peptides were directly loaded onto the analytical column with a maximum flow rate that would not exceed the set pressure limit of 980 bar (usually around 0.8 – 1.0 µL/min). Peptides were subsequently separated on the analytical column by running a 70 min gradient of solvent A and solvent B (start with 7% B; gradient 7% to 35% B for 60 min; gradient 35% to 100% B for 5 min and 100% B for 5 min) at a flow rate of 300 nl/min. The mass spectrometer was operated using Xcalibur software (version 2.2 SP1.48). The mass spectrometer was set in the positive ion mode. Precursor ion scanning was performed in the Orbitrap analyser (FTMS) in the scan range of m/z 300-1800 and at a resolution of 60000 with the internal lock mass option turned on (lock mass was 445.120025 m/z, polysiloxane; Olsen et al. 2005). Product ion spectra were recorded in a data dependent fashion in the

ion trap (ITMS) in a variable scan range and at a rapid scan rate. The ionization potential (spray voltage) was set to 1.8 kV. Peptides were analysed using a repeating cycle consisting of a full precursor ion scan (1.0 × 106 ions or 50 ms) followed by 12 product ion scans (1.0 × 104 ions or 100 ms) where peptides are isolated based on their intensity in the full survey scan (threshold of 500 counts) for tandem mass spectrum (MS2) generation that permits peptide sequencing and identification. CID collision energy was set to 35% for the generation of MS2 spectra. During MS2 data acquisition dynamic ion exclusion was set to 120 seconds with a maximum list of excluded ions consisting of 500 members and a repeat count of one. Ion injection time prediction, preview mode for the FTMS, monoisotopic precursor selection and charge state screening were enabled. Only charge states higher than 1 were considered for fragmentation.

Peptide and Protein Identification using MaxQuant. RAW spectra were submitted to an Andromeda (Cox et al. 2011) search in MaxQuant (version 1.5.3.30) using the default settings (Cox und Mann 2008). Label-free quantification and match-between-runs was activated (Cox et al. 2014). MS/MS spectra data were searched against the *Xenopus laevis* (African clawed frog, taxonomy-id: 8355) database downloaded from Uniprot (16460 entries) which was supplemented with the human p97 VCP sequence (Uniprot id: P55072). All searches included a contaminants database (as implemented in MaxQuant, 267 sequences). The contaminants database contains known MS contaminants and was included to estimate the level of contamination. Andromeda searches allowed oxidation of methionine residues (16 Da) and acetylation of the protein N-terminus (42 Da) as dynamic modifications and the static modification of cysteine (57 Da, alkylation with iodoacetamide). Enzyme specificity was set to “Trypsin/P”. The instrument type in Andromeda searches was set to Orbitrap and the precursor mass tolerance was set to ±20 ppm (first search) and ±4.5 ppm (main search). The MS/MS match tolerance was set to ±0.5 Da. The peptide spectrum match FDR and the protein FDR were set to 0.01 (based on target-decoy approach). Minimum peptide length was 7 amino acids. For protein quantification unique and razor peptides were allowed. Modified peptides were allowed for quantification. The minimum score for modified peptides was 40.

Data Analysis. The list of identified proteins generated by MaxQuant was loaded into Perseus (version 1.5.2.6). First, proteins were excluded, if they were flagged by MaxQuant as “contaminants”, “reverse” or “only identified by site”. Then, the LFQ intensities were logarithmised and grouped in quadruplicates. The list was filtered for proteins with at least four valid values (i.e. in all replicates) in at least one group. After this, missing values were imputed with values representing a normal distribution around the detection range of the mass spectrometer. For this, mean and standard deviation of the measured intensities were determined and a new distribution with a downshift of 1.8 standard deviations and a width of 0.3 standard deviations was generated. The total matrix was imputed using these values. The differences of the logarithmised means of the two groups (SB-DNA beads with and without ND1) and the negative logarithmised p values were displayed as volcano plot in Figure 1A. To correct for multiple testing, a permutation-based false discovery rate (FDR) approach was applied using an FDR of 5% and an s0 of 0.1.

Supplemental References

Britton, Sébastien; Coates, Julia; Jackson, Stephen P. (2013): A new method for high-resolution imaging of Ku foci to decipher mechanisms of DNA double-strand break repair. In: *J Cell Biol* 202 (3), S. 579–595. DOI: 10.1083/jcb.201303073.

Carpenter, A. E.; Jones, T. R.; Lamprecht; Clarke, C.; Kang, I. H.; Friman, O. et al. (2006): CellProfiler: image analysis software for identifying and quantifying cell phenotypes. In: *Genome biology* 7 (10), S. R100. DOI: 10.1186/gb-2006-7-10-r100.

Certo, Michael T.; Ryu, Byoung Y.; Annis, James E.; Garibov, Mikhail; Jarjour, Jordan; Rawlings, David J.; Scharenberg, Andrew M. (2011): Tracking genome engineering outcome at individual DNA breakpoints. In: *Nature methods* 8 (8), S. 671–676. DOI: 10.1038/nmeth.1648.

Cox, J.; Hein, M. Y.; Luber, C. A.; Paron, I.; Nagaraj, N.; Mann, M. (2014): Accurate proteome-wide label-free quantification by delayed normalization and maximal peptide ratio extraction, termed MaxLFQ. In: *Molecular & cellular proteomics : MCP* 13 (9), S. 2513–2526. DOI: 10.1074/mcp.M113.031591.

Cox, J.; Mann, M. (2008): MaxQuant enables high peptide identification rates, individualized p.p.b.-range mass accuracies and proteome-wide protein quantification. In: *Nature biotechnology* 26 (12), S. 1367–1372. DOI: 10.1038/nbt.1511.

Cox, J.; Neuhauser, N.; Michalski, A.; Scheltema, R. A.; Olsen, J. V.; Mann, M. (2011): Andromeda: a peptide search engine integrated into the MaxQuant environment. In: *Journal of proteome research* 10 (4), S. 1794–1805. DOI: 10.1021/pr101065j.

Dobrynin, G.; Popp, O.; Romer, T.; Bremer, S.; Schmitz, M. H. A.; Gerlich, D. W.; Meyer, H. (2011): Cdc48/p97-Ufd1-Npl4 antagonizes Aurora B during chromosome segregation in HeLa cells. In: *Journal of Cell Science* 124 (9), S. 1571–1580. DOI: 10.1242/jcs.069500.

Funabiki, H.; Murray, A. W. (2000): The Xenopus chromokinesin Xkid is essential for metaphase chromosome alignment and must be degraded to allow anaphase chromosome movement. In: *Cell* 102 (4), S. 411–424.

Gunn, Amanda; Bennardo, Nicole; Cheng, Anita; Stark, Jeremy M. (2011): Correct end use during end joining of multiple chromosomal double strand breaks is influenced by repair protein RAD50, DNA-dependent protein kinase DNA-PKcs, and transcription context. In: *The Journal of biological chemistry* 286 (49), S. 42470–42482. DOI: 10.1074/jbc.M111.309252.

Hetzer, Martin; Meyer, Hemmo H.; Walther, Tobias C.; Bilbao-Cortes, Daniel; Warren, Graham; Mattaj, Iain W. (2001): Distinct AAA-ATPase p97 complexes function in discrete steps of nuclear assembly. In: *Nat. Cell Biol.* 3 (12), S. 1086–1091. DOI: 10.1038/ncb1201-1086.

Ismail, Ismail Hassan; Gagné, Jean-Philippe; Genois, Marie-Michelle; Strickfaden, Hilmar; McDonald, Darin; Xu, Zhizhong et al. (2015): The RNF138 E3 ligase displaces Ku to promote DNA end resection and regulate DNA repair pathway choice. In: *Nat Cell Biol* 17 (11), S. 1446–1457. DOI: 10.1038/ncb3259.

Meerang, Mayura; Ritz, Danilo; Paliwal, Shreya; Garajova, Zuzana; Bosshard, Matthias; Mailand, Niels et al. (2011): The ubiquitin-selective segregase VCP/p97 orchestrates the response to DNA double-strand breaks. In: *Nat Cell Biol* 13 (11), S. 1376–1382. DOI: 10.1038/ncb2367.

Meyer, Hemmo H.; Shorter, James G.; Seemann, Joachim; Pappin, Darryl; Warren, Graham (2000): A complex of mammalian Ufd1 and Npl4 links the AAA-ATPase, p97, to ubiquitin and nuclear transport pathways. In: *EMBO J* 19 (10), S. 2181–2192. DOI: 10.1093/emboj/19.10.2181.

Michalski, A.; Damoc, E.; Lange, O.; Denisov, E.; Nolting, D.; Muller, M. et al. (2012): Ultra high resolution linear ion trap Orbitrap mass spectrometer (Orbitrap Elite) facilitates top down LC MS/MS and versatile peptide fragmentation modes. In: *Molecular & cellular proteomics : MCP* 11 (3), S. O111.013698. DOI: 10.1074/mcp.O111.013698.

Olsen, J. V.; Godoy, L. M. de; Li, G.; Macek, B.; Mortensen, P.; Pesch, R. et al. (2005): Parts per million mass accuracy on an Orbitrap mass spectrometer via lock mass injection into a C-trap. In: *Molecular & cellular proteomics : MCP* 4 (12), S. 2010–2021. DOI: 10.1074/mcp.T500030-MCP200.

Park, M. Y.; Moon, J. H.; Lee, K. S.; Choi, H. I.; Chung, J.; Hong, H. J.; Kim, E. (2007): FAF1 suppresses IkappaB kinase (IKK) activation by disrupting the IKK complex assembly. In: *The Journal of biological chemistry* 282 (38), S. 27572–27577. DOI: 10.1074/jbc.C700106200.

Postow, Lisa; Funabiki, Hironori (2014): An SCF complex containing Fbxl12 mediates DNA damage-induced Ku80 ubiquitylation. In: *Cell Cycle* 12 (4), S. 587–595. DOI: 10.4161/cc.23408.

Postow, Lisa; Ghenoiu, Cristina; Woo, Eileen M.; Krutchinsky, Andrew N.; Chait, Brian T.; Funabiki, Hironori (2008): Ku80 removal from DNA through double strand break–induced ubiquitylation. In: *J Cell Biol* 182 (3), S. 467–479. DOI: 10.1083/jcb.200802146.

Raman, Malavika; Havens, Courtney G.; Walter, Johannes C.; Harper, J. Wade (2011): A Genome-wide Screen Identifies p97 as an Essential Regulator of DNA Damage-Dependent CDT1 Destruction. In: *Molecular Cell* 44 (1), S. 72–84. DOI: 10.1016/j.molcel.2011.06.036.

Rappsilber, J.; Mann, M.; Ishihama, Y. (2007): Protocol for micro-purification, enrichment, pre-fractionation and storage of peptides for proteomics using StageTips. In: *Nature protocols* 2 (8), S. 1896–1906. DOI: 10.1038/nprot.2007.261.

Wang, Yanzhuang; Satoh, Ayano; Warren, Graham; Meyer, Hemmo H. (2004): VCIP135 acts as a deubiquitinating enzyme during p97–p47-mediated reassembly of mitotic Golgi fragments. In: *J Cell Biol* 164 (7), S. 973–978. DOI: 10.1083/jcb.200401010.

Wojcik, Cezary; Yano, Mihiro; DeMartino, George N. (2004): RNA interference of valosin-containing protein (VCP/p97) reveals multiple cellular roles linked to ubiquitin/proteasome-dependent proteolysis. In: *Journal of Cell Science* 117 (Pt 2), S. 281–292. DOI: 10.1242/jcs.00841.

Zhou, Hua-Lin; Geng, Cuiyu; Luo, Guangbin; Lou, Hua (2013): The p97-UBXD8 complex destabilizes mRNA by promoting release of ubiquitinated HuR from mRNP. In: *Genes & development* 27 (9), S. 1046–1058. DOI: 10.1101/gad.215681.113.